Actin microridges characterized by laser scanning confocal and atomic force microscopy

Amita Sharma, Kurt I. Anderson, Daniel J. Müller*

BIOTEC and Max-Planck-Institute of Molecular Cell Biology and Genetics, 01307 Dresden, Germany

Received 16 November 2004; revised 3 February 2005; accepted 21 February 2005

Available online 8 March 2005

Edited by Amy McGough

Abstract **We have characterized the cell surface of zebrafish stratified epithelium using a combined approach of light and atomic force microscopy under conditions which simulate wound healing. Microridges rise on average 100 nm above the surface of living epithelial cells, which correlate to bundles of cytochalasin B-insensitive actin filaments. Time-lapse microscopy revealed the bundles to form a highly dynamic network on the cell surface, in which bundles and junctions were severed and annealed on a time scale of minutes. Atomic force microscopy topographs further indicated that actin bundle junctions identified were of two types: overlaps and integrated end to side T- and Y-junctions. The surface bundle network is found only on the topmost cell layer of the explant, and never on individual locomoting cells. Possible functions of these actin bundles include cell compartmentalization of the cell surface, resistance to mechanical stress, and F-actin storage.**

Keywords: Actin cytoskeleton; Atomic force microscopy; Cell membrane; Light microscopy; Stratified epithelium

1. Introduction

Progress in cell biology has been driven by the development of new research tools. Electron micrographs of cells taken by Porter [1] in the 1940s were crude by today's standards, but represented the birth of what would become a powerful tool for cell biological research. Early pharmacological tools such as the cytochalasins were extensively used to disrupt microfilaments [2] even before their mode of action was fully understood [3,4]. Pharmacological progress since then has generated an impressive toolbox for selectively interfering with many steps of F-actin equilibrium. Fluorescence microscopy techniques have progressed from immuno-cytochemistry of fixed preparations to advanced techniques of photo-bleaching, photo-activation, and fluorescent protein technology, which have driven characterization of actin containing structures and dynamics to the resolution limits of the light microscope.

Atomic force microscopy (AFM) was initially invented to image conductive and non-conductive surfaces at the subnanometer level [5]. The development of the fluid cell has allowed observation of samples in solution, thereby widening the application of AFM to include biological samples [6]. As a surface sensitive technique, it offers distinct advantages and often complementary information over more conventional microscopic techniques. For example, cells and biological material can be observed directly with very little sample preparation and AFM topographs can be obtained at a spatial resolution down to 1 nm. The advantage over electron microscopy is that living cells can be imaged in physiologically relevant solution, providing a platform to observe dynamic biological processes in real time [7–10]. The limited scanning speed of AFM currently presents a bottleneck to observation of dynamic biological processes, which often occur in seconds rather than the minutes required to obtain clear topographs. However, studying cells with AFM also presents other challenges. Many structures of cell surface may be too soft to be imaged successfully by the AFM stylus. The key to achieving a meaningful topograph is to apply force as small as possible to prevent sample distortion [11,12]. Complementary types of information, i.e. surface topography or elasticity revealed by AFM, can be combined with information observed from light microscopy. Such multi modal imaging offers a powerful tool to reveal novel insights into biological systems at high-resolution [13–15].

Individual keratocytes isolated from fish or amphibia have been a useful model for investigation of many aspects of actin dynamics in cell motility, including actin filament treadmilling [16], coordination of protrusion and retraction [17], adhesion [18], force generation [19], and membrane dynamics [20]. Here, we report on the morphology of the zebrafish keratocytes within a confluent, stratified squamous epithelium by combining AFM with time-lapse phase contrast, wide field and laser scanning confocal fluorescence microscopy. Our results substantially confirm and extend earlier electron microscopy studies of the ultra-structure of keratocyte monolayers [21,22]. Here, we reveal new details of the structural and functional nature of dynamic surface ridges established at the outermost layer of keratocytes in tissue.

2. Results

2.1. Cells within a confluent layer express regular surface structures

Fig. 1 shows the typical arrangements of keratocytes observed within a confluent epithelial layer using AFM. Individual cells expressing ridge like structures [22] just below the plasma membrane were interspersed with cells having smooth surfaces (Fig. 1C). The arrangement and density of ridges varied from cell to cell. In some cells they were only present in the

*Corresponding author. Fax: +49 351 463 40342.
E-mail address: daniel.mueller@biotec.tu-dresden.de (D.J. Müller).

0014-5793/$30.00
doi:10.1016/j.febslet.2005.02.049

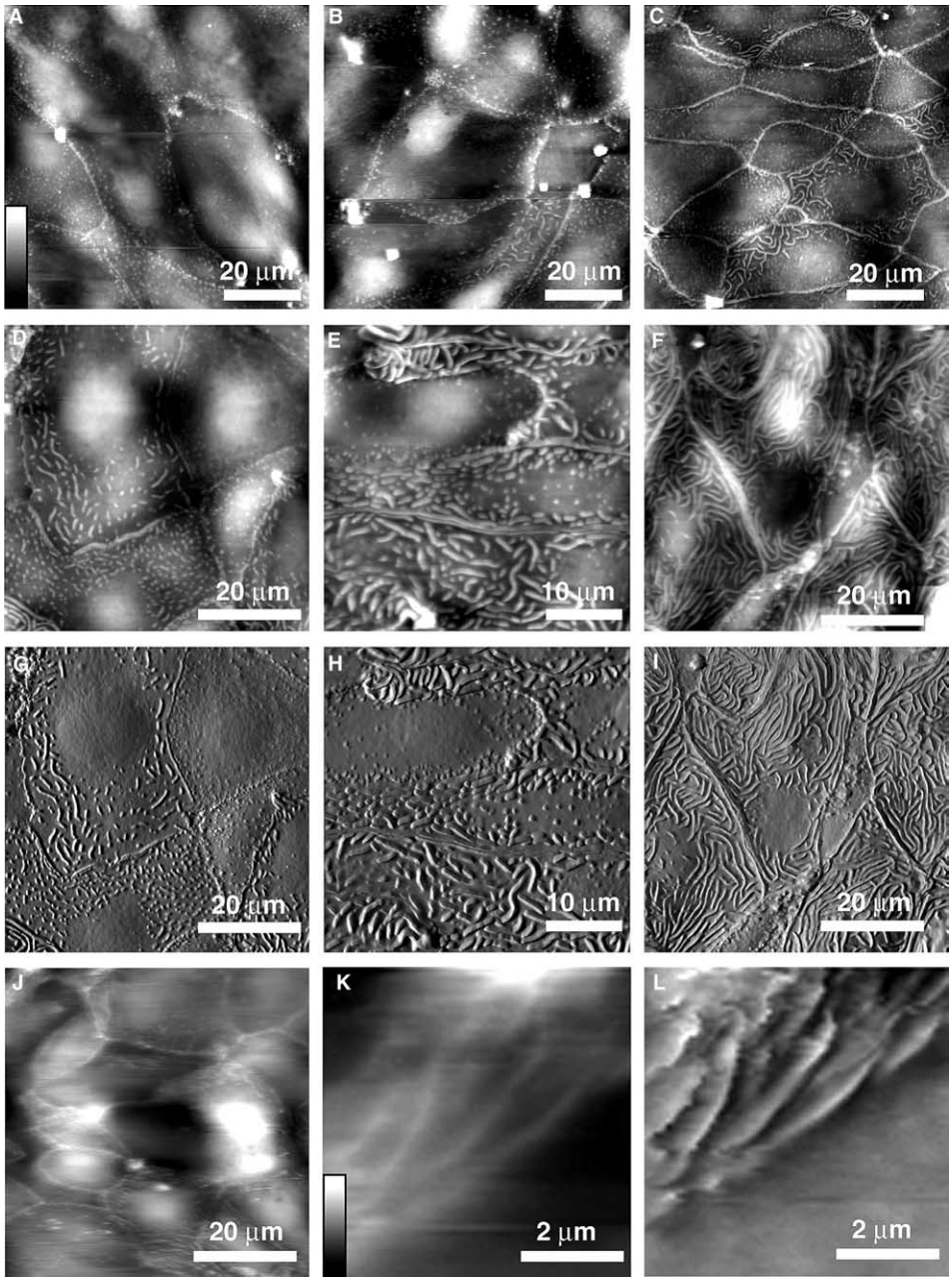

Fig. 1. AFM topographs of keratocyte epithelium. (A) to (F) show the wide variety of length, shape, and distribution among surface structures expressed on keratocytes in the same explant. (G), (H) and (I) show deflection images of (D), (E) and (F), respectively. (J), (K) and (L) are topographs of living cells, which show the appearance of ridges is identical to fixed cells. All topographs were recorded in solution using constant force mode at <50 pN. Note in (D) and (G) the juxtaposition of ridged (left) and flat surfaced cells (right). The gray scales (insets) correspond to vertical heights of 1 μm (A–F and J) and vertical heights of 500 nm (K) of the topographs.

periphery whereas in others they accumulated around the nuclear region; there was no consistent orientation of ridges with respect to the cell margin. Occasionally, they covered the entire cell surface (Fig. 1F). AFM topographs of live cells (Figs. 1J–L) showed similar structures to those observed of fixed specimens, although mobility of the sample posed a challenge to imaging large sample areas.

To record a topograph (512×512 pixels) of a highly modulated surface such as a cell, commercially available AFMs currently require recording times ranging between 20 and 50 min. Because epidermis cells showed a high mobility and their surface structures were highly dynamic in vivo (see below) AFM overview topographs showed blurred surfaces (Fig. 1J). Small areas of the cell surface, which were less modulated could be imaged at imaging times of about 10 min. These topographs allowed observing dynamic cell surface structures in vivo (Figs. 1K and L). However, to obtain overview topographs, the sample had to be fixed before scanning by AFM.

In agreement with previously published reports, keratocytes released from the monolayer, whether canoe or fried egg shaped, did not show any ridges on their surfaces.

From the AFM topographs shown in Fig. 1 it can be seen that the ridges varied in their dimensions, orientation and curvature. An analysis of ridge heights and widths on the surface of living and fixed cells under physiological conditions (Fig. 2) show that they protruded from 20 to 213 nm above the surrounding cell membrane (Figs. 2A and B), exhibiting an average height of 99 ± 34 nm ($n = 200$). Two hundred measurements of ridges randomly selected from five cells taken from different explant cultures prepared on different days showed that their widths at full-width half-maximum ranged from 350 to 780 nm, with an average of 552 ± 106 nm (means ± S.D.; $n = 20$). Forward and backward scanning of the same region indicated that ridges were resilient surface structures.

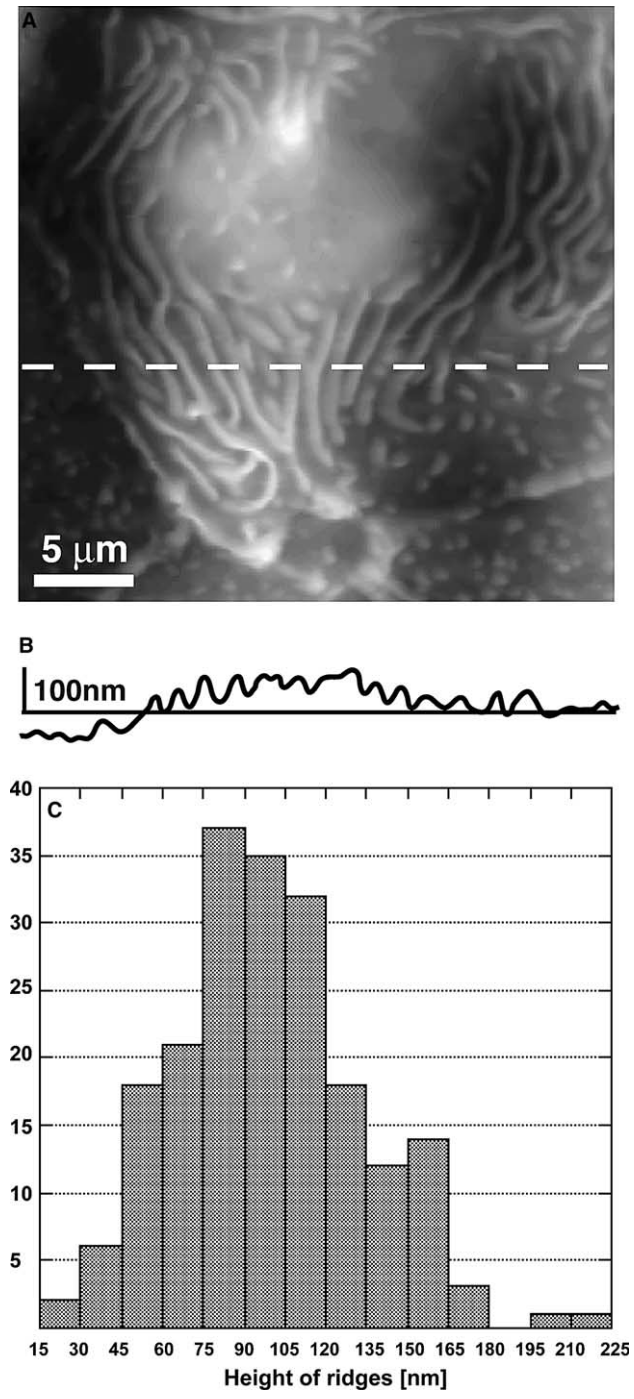

Fig. 2. AFM topograph height analysis. AFM topograph (A) and height trace (B) of individual ridges along the dotted line in (A). Vertical line represents 100 nm. Note that the surface is typically concave due to the thickness of the cell nucleus. (C) Histogram showing the distribution of heights among 200 randomly selected ridges from five cells. The mean height is 99 ± 34 nm.

2.2. Surface structures correlate with actin bundles

In a previous publication it was stated, that the ridges were composed of actin filaments [22]. The question, whether all ridges were composed of F-actin, or whether some of the ridges were established by, for example, microtubuli or intermediate filaments could not be answered unambiguously. To investigate whether all ridges were composed of actin, cells were stained with fluorescently conjugated phalloidin. Wide field fluorescent micrographs and AFM topographs were then recorded of the same cells (Fig. 3). The ridges stained positive for F-actin correlated exactly with the ridge-like structures

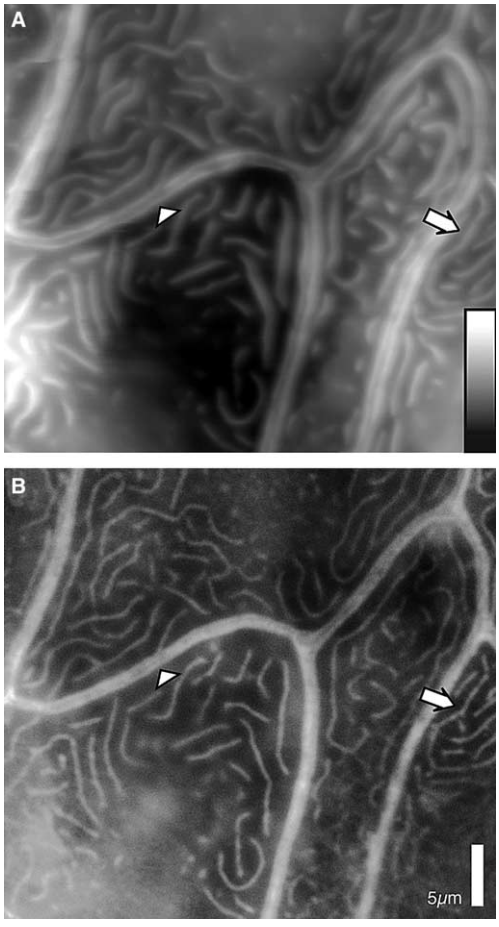

Fig. 3. AFM and fluorescence images of surface ridges. (A) Ridge heights of AFM topography. (B) Fluorescent image of the same region stained with phalloidin, to demonstrate the F-actin composition of the ridges on the cell surface. Arrowheads point out details of cell–cell junctions. In the topograph, the cell junction appears as two ridges each belonging to a different cell. Arrows point to the same ridge in both images. Although individual ridges appear narrower in the fluorescence image, they are better resolved at cell junctions within the AFM image.

observed in the AFM topograph. Thus, every ridge observed on the cell surface contained F-actin. Individual ridges appeared somewhat thinner and sharper in light micrographs. However, in AFM topographs cell–cell junctions can be clearly distinguished as two distinct ridges as little as 100 nm apart, which is beyond the normal resolution limit of the light microscope.

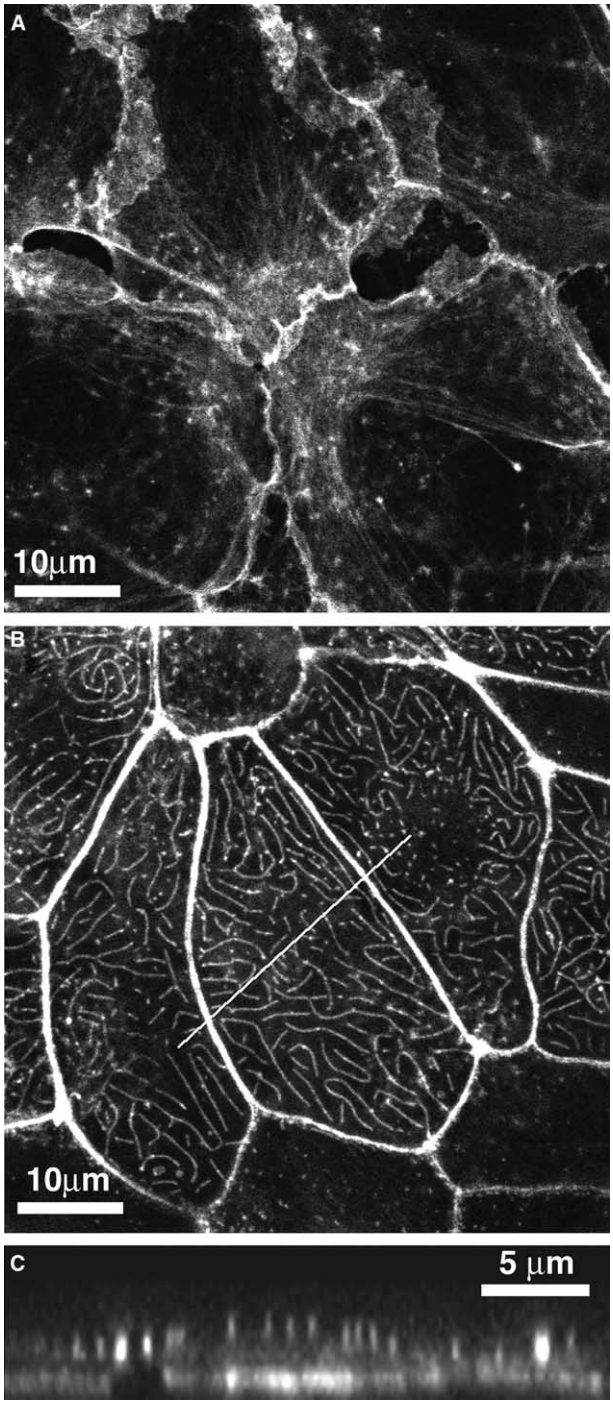

Fig. 4. Fluorescent confocal images showing stratified arrangement of tissue. (A) Lower cell layer attached to the coverslip. Cells appear only partially attached, with lamellipodia extending in some places below other cells or into the space between cells. (B) The upper layer of cells joined by tight junctions, with well developed F-actin bundles. Images represent the sum of three (A) and five (B) consecutive confocal sections. (C) Cross section through the line in (B). The oblong shape of surface bundles along the *z*-axis is due to the point spread function of the confocal microscope.

2.3. Ridge-like structures appeared only on keratocytes on the surface layer

Primary keratocyte explants generally form two distinct, stratified cell layers, similar to the arrangement in vivo [23,24]. Confocal images recorded through the same tissue region showed two cell layers having different morphologies (Fig. 4). The bottom layer consisted of spreading cells with lamellipodia attached to the glass coverslip (Fig. 4A). In contrast, the top layer exhibited no lamellipodia or any sign of active spreading (Fig. 4B). Instead these cells were characterized by pronounced lateral cell–cell junctions, which appeared as a double ridge in AFM. Only the upper cell layer expressed the ridge-like structures of F-actin, which were found in confocal sections to be present on the cell surface facing the buffer solution (Fig. 4C).

2.4. Actin bundles in microridges are insensitive to cytochalasin B treatment

Keratocyte explants were treated with 500 ng/ml cytochalasin B for 5, 10, or 20 min to estimate the treadmilling rate of actin filaments contained within the microridge bundles. Confocal images of the dorsal cell surface revealed no obvious changes in the relative number, size, or length of cortical actin bundles compared to control cells (Fig. 5). In contrast, the lamellipodia of cells at the border of the confluent layer were void of F-actin, indicating the drug concentration was sufficient to promote depolymerization of rapidly treadmilling actin filaments. This indicates that actin filaments within the microridges are not actively treadmilling.

2.5. Time-lapse images reveal dynamic nature of F-actin ridges

The frame rate of AFM proved insufficient to follow the dynamics of the ridges in living cells, so phase contrast time-lapse studies were carried out on confluent layers (Fig. 6). Time-lapse images showed that overall the cells within the monolayer were active and changed shape considerably over a period of 4–5 h. However, ridge behavior was surprisingly dynamic on a time scale of minutes. Ridges changed position independently relative to each other and the cell margin. They appeared to split or merge end to end with other ridges, as well as rapidly form and break T- and Y-shaped intersections. Individual ridges were observed to undergo tight hairpin bends, demonstrating their high elastic resilience. The tissue layers also proved to be highly mobile, with cells drifting across the field of view with an average speed of 2.37 μm/min. Changes in cell shape and position thus made the long term observation of cells and ridge patterns difficult. F-actin ridges could no longer be observed in phase contrast when cells rounded up, however, confocal imaging indicated F-actin bundles remained on the cell surface; i.e., no bundles were seen to internalize and stretch through the centre of rounded up cells.

Phase contrast images suggest that intersecting ridges do not slide relative to each other, i.e., they appeared fixed to each other at points of intersection. AFM topographs suggested

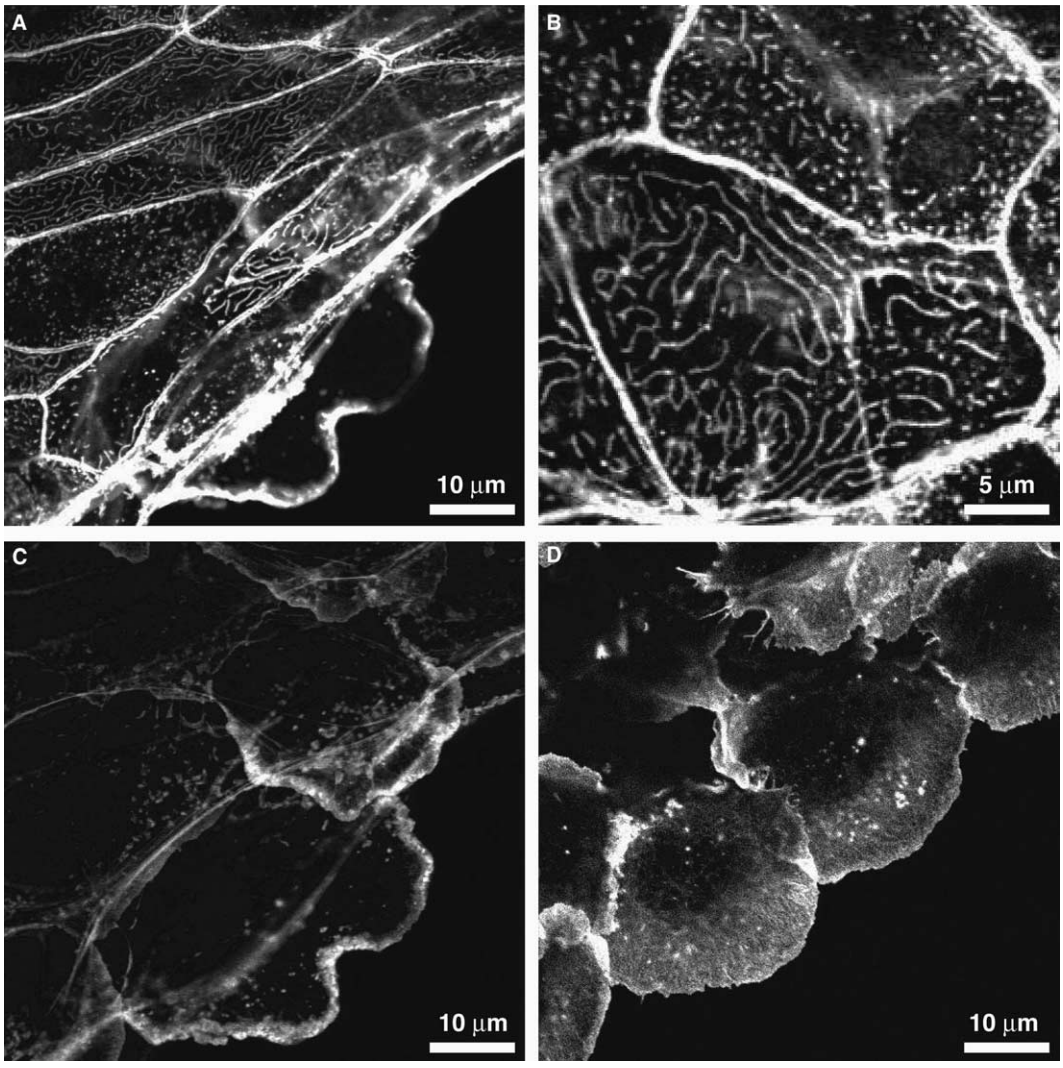

Fig. 5. Confocal sections of cytochalasin treated cells. Keratocytes were treated with 500 ng/ml cytochalasin B for 10 (A, C) or 20 (B) min prior to fixation and staining with fluorescently conjugated phalloidin. (A) and (C) show apical and basal cell surfaces of the same specimen, respectively. (D) Control cells showing normal distribution of actin filaments in lamellipodia in comparison to hollowed out lamellipodia of cytochalasin B treated cells (C). Actively treadmilling actin filaments within lamellipodia are depolymerized (C), whereas actin bundles within microridges resist depolymerization due to drug treatment (A).

two kinds of intersections (Fig. 7). In some cases the actin bundles forming the ridges appeared to simply overlay (arrow 2, Fig. 7). Other traces indicated that junctions could be formed through the integration of the end of one bundle into the side of another (arrow 1, Fig. 7).

3. Discussion

3.1. Combining AFM and light microscopy

We have employed AFM to compliment information obtained from the light microscope to characterize a novel structure of the actin cytoskeleton in fixed and living cells. As a surface sensitive technique AFM is predominantly applied to acquire topographical information, whereas LM, especially confocal, can image deep within cells or tissue. Flat, stratified epithelium proved to be an amenable specimen to both imaging techniques. The low surface ridges present on the outer cell layer were perfectly accessible to the AFM stylus. The vertical resolution achieved in AFM topographs is well beyond that of the confocal microscope, allowing conclusions to be drawn about the proximity of cell membrane and underlying structures which would not be possible with light microscopy alone. Additionally, the lateral resolution of AFM allowed resolving bundle pairs which were generally seen as one broad bundle in confocal images. Topographs of living cells were identical to those of fixed cells, demonstrating that sufficiently low force could be applied on living cells to prevent distortion of the cell surface. Similarly, the height measurements from bundles in live cell AFM topographs were the same as those taken from fixed cells.

The average ridge width of 552 nm as measured by AFM lies about two times higher than the width of ≈300 nm determined by light microscopy [22]. One reason for this broadening can be found in the different types of information measured. AFM as a surface sensitive technique measures the width of the ridges inclusive that of the cell membrane. It is well known, that rough and protruding structures imaged by the AFM

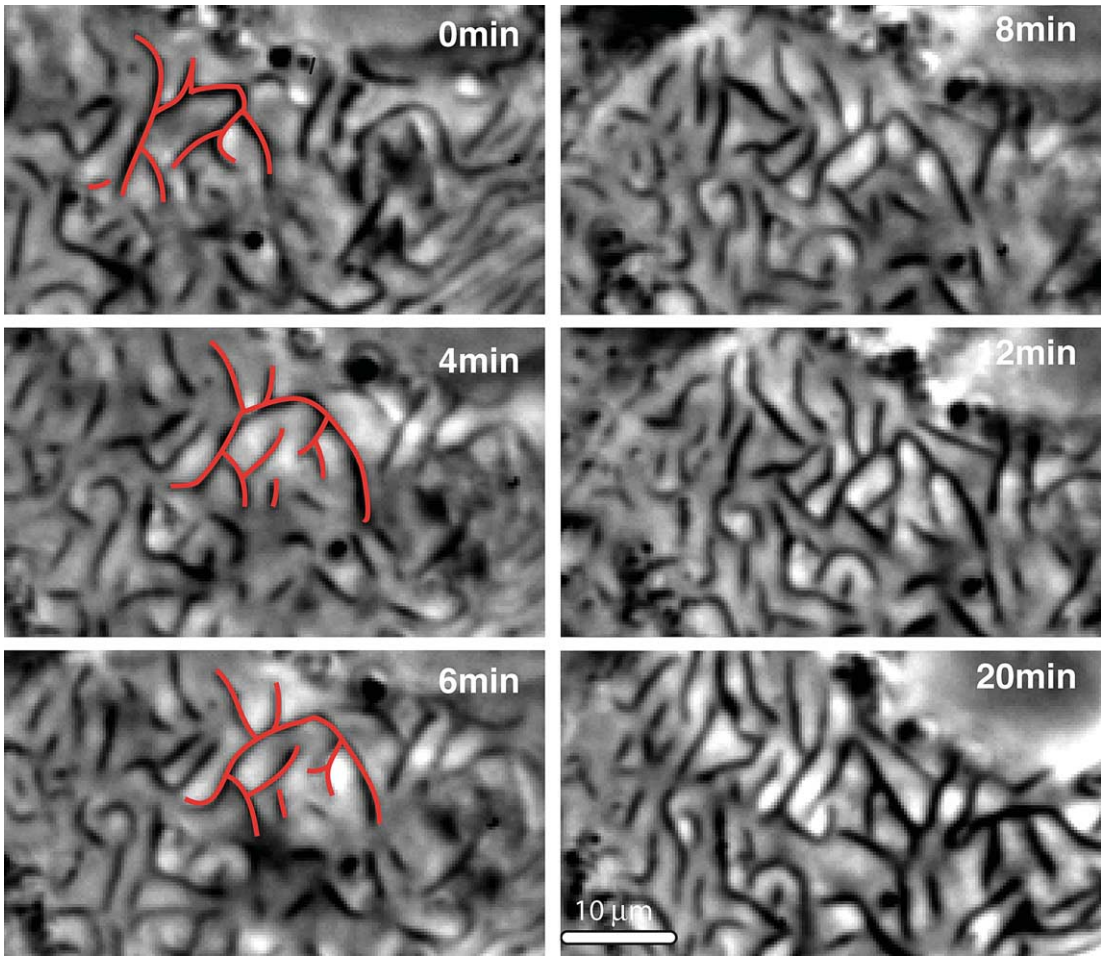

Fig. 6. Phase contrast time series of ridge dynamics within a sub-region of the cell surface. The red outline in the first three frames is provided for orientation. The initial bundle pattern becomes unrecognizable on a time scale of minutes, whereas overall cell shape remains relatively stable during the same period.

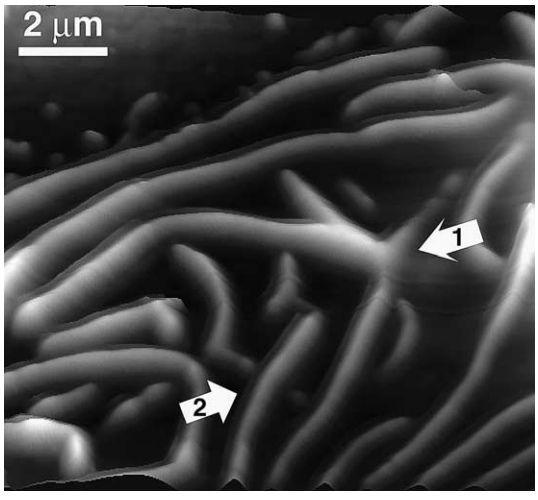

Fig. 7. Intersections of actin bundles structuring the keratocyte membrane. AFM topograph suggesting F-actin ridges to overlap (arrow 2) and to form T-junctions (arrow 1). Topograph is displayed in perspective view and exhibits a vertical scale of 500 nm.

stylus can appear severely broadened due to a non-linear convolution effect [25]. Assuming a pyramidal AFM stylus and that the width of the structures observed were measured at full width half maximum of height (≈50 nm) the broadening effect by the AFM stylus corresponds to almost ≈100 nm. Thus, it may be assumed that the cellular structures wrapping a ridge are ≈25–50 nm thick.

The height differences measured between the cell membrane covering ridges and of the surrounding cell membrane lied between 20 and 200 nm. These values lie, however, much below the heights ranging between 200 and 1000 nm revealed from electron microscopy (EM) data of tissue cultured epidermis cells from female guppies and from sea horses [22]. This discrepancy may have several reasons: firstly, the samples prepared for the transmission electron microscopy experiments were dehydrated and thus the heights measured may not represent that of the native tissue. In this work, the sample preparation and measurements were performed throughout in aqueous solution. Secondly, the tissue cultured epidermis cells investigated by AFM were from zebrafish while those investigated by EM were from different biological organisms: guppy and sea horse. Thirdly, in their work Bereiter-Hahn et al. [22] assume that height variations of microridges may result from different tissue culturing conditions. This leads to the speculation that environmental and growth conditions, the age of the organism, or the sample culture conditions may also influence the expression of microridges, and suggests a biological origin to the variation in heights measured in the two studies.

3.2. Epithelial tissue expresses regular F-actin surface structures

Fish keratocytes have served as a useful model system for the study of actin dynamics in cell motility. Here, we have concentrated on the structure and morphology of cells within spreading tissue, a situation related to wound healing in vivo. AFM topographs revealed the cell surfaces of these explants to be compartmentalized by regular surface structures. These surface structures were only observed on cells within the topmost confluent layer having tight cell–cell junctions. However, it was also observed that not every cell exhibited these structures and that amongst the cells that did, their number and form varied considerably. They are found day 1 of culture and occur randomly in cells throughout the upper cell layer, which has been characterized as non-motile in the wound healing response of *Xenopus* tadpoles [23,24]. These cortical bundles form ridges in the cell surface [22], and represent a unique F-actin structure along side other well characterized forms such as stress fibers, filopodia, and microvilli. Assuming a diameter of about 300 nm, it can be estimated that each bundle might contain several hundred actin filaments in cross section. Further work is required to determine the identities of actin binding proteins organizing the bundles, and the ultra-structure of actin filaments within the bundles.

3.3. Dynamic F-actin surface structures show different types of intersection

Time-lapse light microscopy revealed these F-actin surface structures to be highly dynamic. The fact that they are able to quickly undergo sharp bends suggests that in contrast to stress fibers they are not under tension. They are able to break, anneal, and form junctions on a time scale of minutes. The rapid severing and annealing of ridges poses many questions. AFM topographs clearly indicate two types of intersection. In one case points of intersection between two ridges are not simply one bundle resting on top of the other – differences in position which would be difficult to resolve in the light microscope. Instead bundles merge at the same height through the integration of one bundle into the side of the other. This type of junction is consistent with Arp 2/3 mediated dendritic nucleation of new filaments. The resistance of bundles to cytochalasin treatment demonstrates that actin filaments within the bundles are not actively treadmilling, and suggests that microridges could represent a storage form of F-actin.

The two-dimensional network established by F-actin ridges appeared to be randomly organized. This network may be given more rigidity by welding different ridges to one another (Figs. 1, 4, 6 and 7). Ridges are highly dynamic as demonstrated by bending, instantaneous end-to-end displacements, and lateral mobility even though the contour length of the ridges is expected to be constant. Further studies will show if and how ridges modulate properties of the cell surface in response to environmental changes, metabolism, and external stress.

The nature of the bundle re-arrangements beneath the cell surface poses further questions. Are these rearrangements caused passively by changes in cell shape, or are they driven by motors? It is likely that the bundles are associated with the cortical actin meshwork of the plasma membrane, and that their sliding beneath the cell surface involves the severing and formation of cross linkages between actin filaments. This is supported by the observation in confocal images that when cells round up the bundles remained associated with the cell surface; i.e., they do not collapse into the middle of the cell.

3.4. Possible functions of actin microridges

What is the likely function of these cortical bundles of F-actin? Like microvilli, they are dynamic structures, which constantly change shape [26]. However, based on their relative number, height and orientation parallel to the cell surface these cortical bundles can only marginally increase the surface area of the cell. It is possible that these bundles beneath the cell surface represent a stable, pre-polymerized supply of F-actin, which could be rapidly remodeled for the function of motility [27]. This hypothesis is particularly supported by the observation that motile cells do not posses these surface bundles. Considering the cell location on the outer fish surface, and the location of the bundles on the outer cell surface, we suggest that they may have another function: supporting the plasma membrane and increasing resilience of the cell to physical stress. Further investigation with AFM will allow quantification of cell surface stiffness to test this hypothesis.

4. Materials and methods

4.1. Cell culture

Primary cell cultures of keratocytes were prepared from the scales of zebrafish as described [28]. Culture dishes with well spread confluent layers were selected for AFM imaging.

4.2. Fixation

Before imaging with AFM cells were fixed in 0.1% glutaraldehyde/PBS for 45 s followed by incubation with 3% paraformaldehyde/PBS for 20 min. After this, the samples were gently washed and stored in PBS. For actin staining the cells were permeabilized with 0.5% Triton X-100 and subsequently incubated overnight at 10 °C with Alexa 488-phalloidin (Molecular Probes), diluted 1:1000 in PBS from manufacturers stock.

4.3. Cytochalasin B incubation

Live cell layers were incubated with cytochalasin B at a concentration 500 ng/ml in 'start media' for 0, 5, 10, 15 and 20 min prior to fixation. After this, the actin was stained with phalloidin and imaged by fluorescence confocal microscopy.

4.4. Microscopy

AFM. Live and fixed cells were imaged in PBS using either a Bioscope (Digital Instruments, Santa Barbara) or a NanoWizard (JPK Instruments, Berlin). Both AFMs were mounted on an Axiovert 200M (Zeiss, Germany). Silicon nitride non-sharpened cantilevers used had a nominal force constant of 0.06 N/m (Digital Instruments). Imaging was performed using constant force mode. The thermal drift of the applied force (≈50 pN) was corrected manually during scanning. Line scan rates varied from 0.2 to 0.7 Hz.

Fluorescence microscopy. Wide field imaging of Alexa 488-phalloidin stained cells was performed using the AFM/Axiovert system using a 100×, 1.3 NA Plan Neofluar oil immersion objective. The software used to operate the CCD camera (Cool snap, Visitron systems) was MetaMorph (Universal Imaging Corp.). Confocal laser scanning microscopy was performed using an LSM 510 Meta (Zeiss). The LSM was equipped with a 60×, 1.4 NA Plan Apochromat oil immersion objective. Image stacks in z-direction were acquired through regions having two cell layers. Image J software was used to produce composite images containing only the frames showing each cell layer.

Time-lapse images. An Olympus IX70 microscope, equipped with a 60× PH 3 oil immersion objective (NA 1.25), was used to image live cells within the confluent layer. Phase contrast studies were carried out on live cells within the confluent layer in start media. Time-lapse sequences were also recorded after the start media was substituted with 'Keratocyte Running Buffer' (100 mM NaCl, 20 mM KCl, 0.05 mM $CaCl_2$, 0.05 mM $Ca(NO_3)_2$, 1 mM $NaHCO_3$, 0.8 mM $MgSO_4{\cdot}6H_2O$, and 2 mM PIPES). The Keratocyte Running Buffer disrupted the cell–cell junctions and reversibly separated individual cells from the confluent layer.

Acknowledgments: We thank K. Poole for assistance and critical discussion, T. Reichert-Müller for critical reading, and I. Weisswange for preparing cells. This work was supported by the European Community and the State of Saxony.

References

[1] Porter, K.R., Claude, A. and Fullam, E. (1945) A study of tissue culture cells by electron microscopy. J. Exp. Med. 81, 233–246.
[2] Wessells, N.K., Spooner, B.S., Ash, J.F., Bradley, M.O., Luduena, M.A., Taylor, E.L., Wrenn, J.T. and Yamada, K.M. (1971) Microfilaments in cellular and developmental processes. Science 171, 135–143.
[3] Bray, D. (1979) Cytochalasin action. Nature 282, 671.
[4] Brenner, S.L. and Korn, E.D. (1979) Substoichiometric concentrations of cytochalasin D inhibit actin polymerization. Additional evidence for an F-actin treadmill. J. Biol. Chem. 254, 9982–9985.
[5] Binnig, G., Quate, C.F. and Gerber, C. (1986) Atomic force microscope. Phys. Rev. Lett. 56, 930–933.
[6] Drake, B., et al. (1989) Imaging crystals, polymers, and processes in water with the atomic force microscope. Science 243, 1586–1588.
[7] Engel, A. and Müller, D.J. (2000) Observing single biomolecules at work with the atomic force microscope. Nat. Struct. Biol. 7, 715–718.
[8] Le Grimellec, C., Lesniewska, E., Giocondi, M.C., Finot, E., Vie, V. and Goudonnet, J.P. (1998) Imaging of the surface of living cells by low-force contact-mode atomic force microscopy. Biophys. J. 75, 695–703.
[9] Grandbois, M., Clausen-Schaumann, H. and Gaub, H. (1998) Atomic force microscope imaging of phospholipid bilayer degradation by phospholipase A2. Biophys. J. 74, 2398–2404.
[10] Schneider, S.W., Sritharan, K.C., Geibel, J.P., Oberleithner, H. and Jena, B.P. (1997) Surface dynamics in living acinar cells imaged by atomic force microscopy: identification of plasma membrane structures involved in exocytosis. Proc. Natl. Acad. Sci. USA 94, 316–321.
[11] Henderson, E., Haydon, P.G. and Sakaguchi, D.S. (1992) Actin filament dynamics in living glial cells imaged by atomic force microscopy. Science 257, 1944–1946.
[12] Müller, D.J., Büldt, G. and Engel, A. (1995) Force-induced conformational change of bacteriorhodopsin. J. Mol. Biol. 249, 239–243.
[13] Rotsch, C., Jacobson, K. and Radmacher, M. (1999) Dimensional and mechanical dynamics of active and stable edges in motile fibroblasts investigated by using atomic force microscopy. Proc. Natl. Acad. Sci. USA 96, 921–926.
[14] Rotsch, C. and Radmacher, M. (2000) Drug-induced changes of cytoskeletal structure and mechanics in fibroblasts: an atomic force microscopy study. Biophys. J. 78, 520–535.
[15] Meixner, A.J. and Kneppe, H. (1998) Scanning near-field optical microscopy in cell biology and microbiology. Cell Mol. Biol. (Noisy-le-grand) 44, 673–688.
[16] Theriot, J.A. and Mitchison, T.J. (1991) Actin microfilament dynamics in locomoting cells. Nature 352, 126–131.
[17] Anderson, K.I., Wang, Y.-L. and Small, J.V. (1996) Coordination of protrusion and translocation of the keratocyte involves rolling of the cell body. J. Cell Biol. 134, 1209–1218.
[18] Anderson, K.I. and Cross, R. (2000) Contact dynamics during keratocyte motility. Curr. Biol. 10, 253–260.
[19] Oliver, T., Dembo, M. and Jacobson, K. (1999) Separation of propulsive and adhesive traction stresses in locomoting keratocytes. J. Cell Biol. 145, 589–604.
[20] Kucik, D.F., Elson, E.L. and Sheetz, M.P. (1990) Cell migration does not produce membrane flow. J. Cell Biol. 111, 1617–1622.
[21] Bereiter-Hahn, J. (1971) Light and electron microscopic studies on function of tonofilaments in teleost epidermis. Cytobiologie 4, 73–102.
[22] Bereiter-Hahn, J., Osborn, M., Weber, K. and Voeth, M. (1979) Filament organisation and formation of microridges at the surface of fish epidermis. J. Ultrastruct. Res. 69, 316–330.
[23] Radice, G.P. (1980) Locomotion and cell-substratum contacts of *Xenopus* epidermal cells in vitro and in situ. Journal of Cell Science 44, 201–223.
[24] Radice, G.P. (1980) The spreading of epithelial cells during wound closure in *Xenopus*. Dev. Biol. 76, 26–46.
[25] Schwarz, U.D., Haefke, H., Reimann, P. and Guntherodt, H.J. (1994) Tip artefacts in scanning force microscopy. J. Microsc. 173, 183–197.
[26] Gorelik, J., et al. (2003) Dynamic assembly of surface structures in living cells. Proc. Natl. Acad. Sci. USA 100, 5819–5822.
[27] Machesky, L.M. (1997) Cell motility: complex dynamics at the leading edge. Curr. Biol. 7, R164–R167.
[28] Anderson, K. and Small, J.V. (1998) (Celis, J.E., Ed.), Cell Biology: A Laboratory Handbook, Vol. 2, pp. 372–376, Academic Press, San Diego.